Contribution to induction motor control for electric traction based on intelligent techniques

Zairi Raid(1)**- Salmi Salah**(1)

(1) *Transport and Environment Engineering laboratory, University of the Mentouri brothers Constantine-1.*
E-Mails: raidzairi2901@gmail.com,

ABSTRACT— **The negative impact of CO2 emissions from diesel is forcing the electrification of rail systems to reduce gas emissions. In the case of electric traction the induction motor is considered in many applications as the best solution. This paper presents an intelligent strategy to improve the control performance of the asynchronous motor in a railway traction chain. The technique used to control this motor is IFOC because of its good suitability on the one hand its robustness, of which speed, torque and flux play an essential role in terms of the dynamic parameters of the system. The maximum torque and efficiency are obtained by controlling the speed by the conventional PI controller and that of fuzzy logic and neural network. The simulation results obtained by Matlab/Simulink show that the artificial intelligence ensures the best performance in terms of robustness, stability and fidelity during the sudden variation of the speed and torque.**

KEY-WORDS—**Railway Traction Chain, IFOC, Artificial intelligence, machine, Simulation**

1 Introduction

Nowadays, the development in electric railway traction with induction motor operating at different frequencies, particularly with controlled voltage supply. Including powered voltage-controlled, has increased significantly owing to the technological evolution of static converters associated with control systems as well as signal processors which allow the real-time processing of complex control algorithms [1].

Induction motors (IM) are widely used as actuators for industrial applications due to their reliability, ruggedness and relatively low maintenance cost [2]. Again presence of inherent coupling effect between the torque and flux of an induction motor makes the control strategy nonlinear and motor's response becomes slow [3]. For this reason, many control techniques were developed to enable decoupling the torque and the flux, in order to control the torque and the flux independently, as in DC motors. Among these methods, we reference the IFOC established by Blaschke [4].

IFOC is commonly used with proportional-integral (PI) or proportional-integral-derivative (PID) controllers, however, in some cases, when the dynamics of the system changes with time or with operating conditions, the performance of the PI is decreased and the control quality is deteriorated (as the gains is fixed in all operating conditions). Fuzzy logic and neural networks are said to be intelligent, used to overcome the above drawbacks. This paper focused on a comparison between three control techniques for an induction motor, PI, fuzzy logic and neural network studied in numerical simulation software (Matlab/Simulink).

2 Induction motor modeling

The dynamics of the induction motor is complex because of the coupling between the stator and the rotor, especially when the coupling coefficients vary with the rotor position. In this model the real three-phase induction motor is replaced by a fictitious, but magnetically equivalent, two-phase machine, due to the Park transformation which allows the transition from a three-phase system (a, b, c) to a system (d, q, h), and certain simplifying assumptions [5].

The analytical study of an induction motor using Park's transformation requires the use of a reference frame that reduces the number of quantities that need to be known in order to simulate the operation of the machine. For this work, we have chosen the stator frame of reference because it is better suited to our study.

2.1 Voltage-fed Asynchronous Machine Model:

The model of the voltage-fed induction motor for a reference frame linked to the stator in a Park reference frame is given by the following electrical equations:

Stator :

$$\begin{cases} V_{sd} = R_s I_{sd} + \frac{d}{dt}\psi_{sd} & (1) \\ V_{sq} = R_s I_{sq} + \frac{d}{dt}\psi_{sq} & (2) \end{cases}$$

Rotor :

$$\begin{cases} V_{rd} = 0 = R_r I_{rd} + \frac{d}{dt}\psi_{rd} - \omega_r \psi_{rq} & (3) \\ V_{rq} = 0 = R_r I_{rq} + \frac{d}{dt}\psi_{rq} - \omega_r \psi_{rd} & (4) \end{cases}$$

Equations du flux :

Stator :

$$\begin{cases} \psi_{sd} = L_s I_{sd} + I_{rd} M & (5) \\ \psi_{sq} = L_s I_{sq} + I_{rq} M & (6) \end{cases}$$

Rotor :

$$\begin{cases} \psi_{rd} = L_r I_{rd} + I_{sd} M & (7) \\ \psi_{rq} = L_r I_{rq} + I_{sq} M & (8) \end{cases}$$

The equation of motion, linking the electrical and mechanical parts is written as follows:

$$j\frac{d\Omega_r}{dx} = T_e - T_r \qquad (9)$$

Torque equation :

$$T_e = \frac{PM}{L_r}.\left(\psi_{rd}.I_{sq} - \psi_{rq}.I_{sd}\right) \quad (10)$$

3 Rotor flux orientation control

The orientation of the stator flux and the air gap flux does not give good performance compared to the orientation of the rotor flux, which gives high torque but requires adaptation of the rotor parameters (which vary with temperature and frequency) [6].

In this case the rotor flux vector control that we implement is based on an orientation of the rotating frame of reference of axes (d, q) such that the d-axis is coincident with the direction of ψr. The flux ψ_r being oriented on the d-axis [7], Thus, the consequences ($\psi_r = \psi_{rd}, \psi_{rq} = 0$) are injected into the model equations to obtain the control and autopilot laws.

In this work, we will adopt an indirect control strategy by orientation of the rotor flow with position or speed sensor at the rotor, necessary to carry out the changes of coordinates.

Therefore, the motor is powered by a voltage inverter, and the control is operated using the pulse width modulation technique. In this case, the control variables are V_{sd} and V_{sq}.

State variables: i_{sd} , i_{sq} , ψ_{rd} et ψ_{rq}

Control variables: V_{sd} et V_{sq}

3.1 Rotor flux equation system

$$V_{sd} = \sigma L_s \frac{di_{sd}}{dt} + R_s i_{sd} - \omega_s \sigma L_s i_{sq} + \frac{M}{L_r}\frac{d}{dt}\psi_r \quad (11)$$

$$V_{sq} = \sigma L_s \frac{di_{sq}}{dt} + R_s i_{sq} + \omega_s \sigma L_s i_{sd} + \omega_s \frac{M}{L_r}\psi_r \quad (12)$$

$$\frac{d}{dt}\psi_r = \frac{M}{T_r} i_{sd} \quad (13)$$

$$T_e = \frac{PM}{L_r}\psi_r i_{sq} \quad (14)$$

$$\omega_r = \frac{M}{T_r}\frac{i_{sq}}{\psi_r} \quad (15)$$

$$j\frac{d\Omega_r}{dx} = T_e - T_r - f\Omega_r \quad (16)$$

For decoupling, we are interested in the compensation technique, which appears to be the simplest because it consists of adding decoupling terms on each of the axes, but with opposite signs.

4 Regulation

4.1 Application of regulator PI to the induction motor

In our work, we used the PI corrector of the proportional-integral action PI which is very widespread in the field of the control of the electric machines and its simplicity of implementation [5].Subsequently the simulation, the calculations of the coefficients (the gains) of the PI controller made by the method of pole compensation at the level of speed control as well as the stator currents (isd, isq), Unfortunately, the calculations did not give enough accuracy to put exact values, where we therefore had to adopt another method that works by the experimental, called the method of Nicole Ziegler. For this, the simulation is performed with the following parameters:

Table 1: Controller parameters used.

Regulator	Kp	Ki
Speed	200	0.5
current (d axis)	10	6000
current (q axis)	5.10	484.21

Fig. 1 present the block diagram of the simulation of an induction motor controlled by the IFOC technique and with the PI controller.

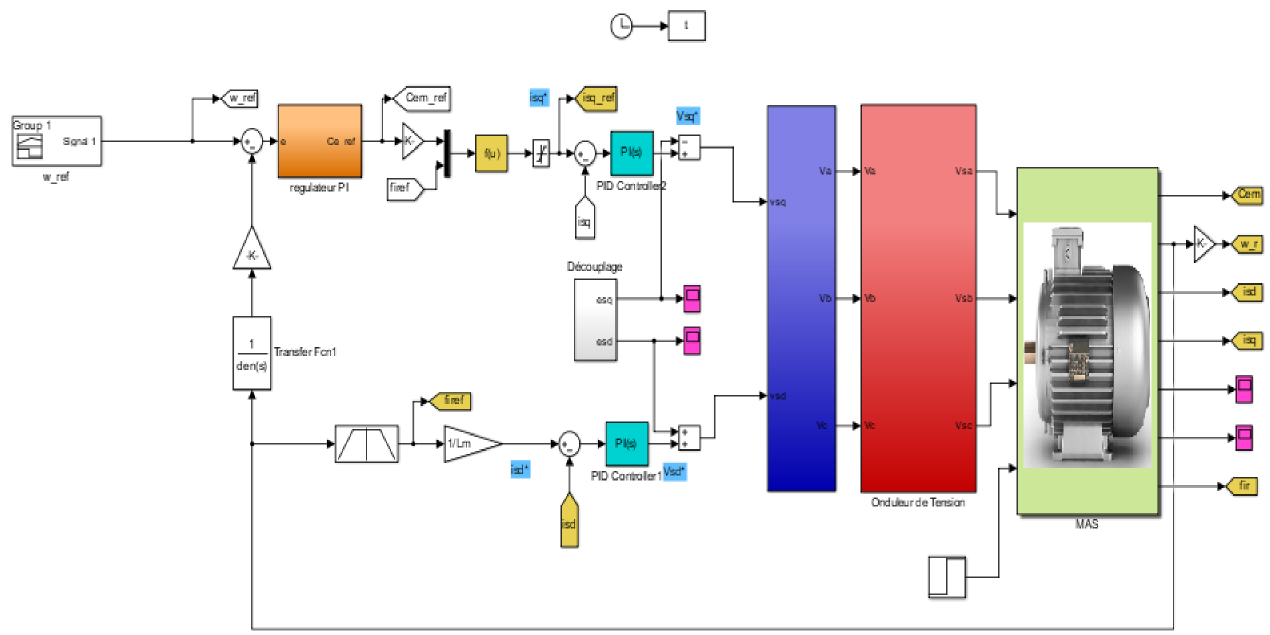

Fig. 1 Block diagram of an Induction motor controlled by the IFOC technique and with PI controller.

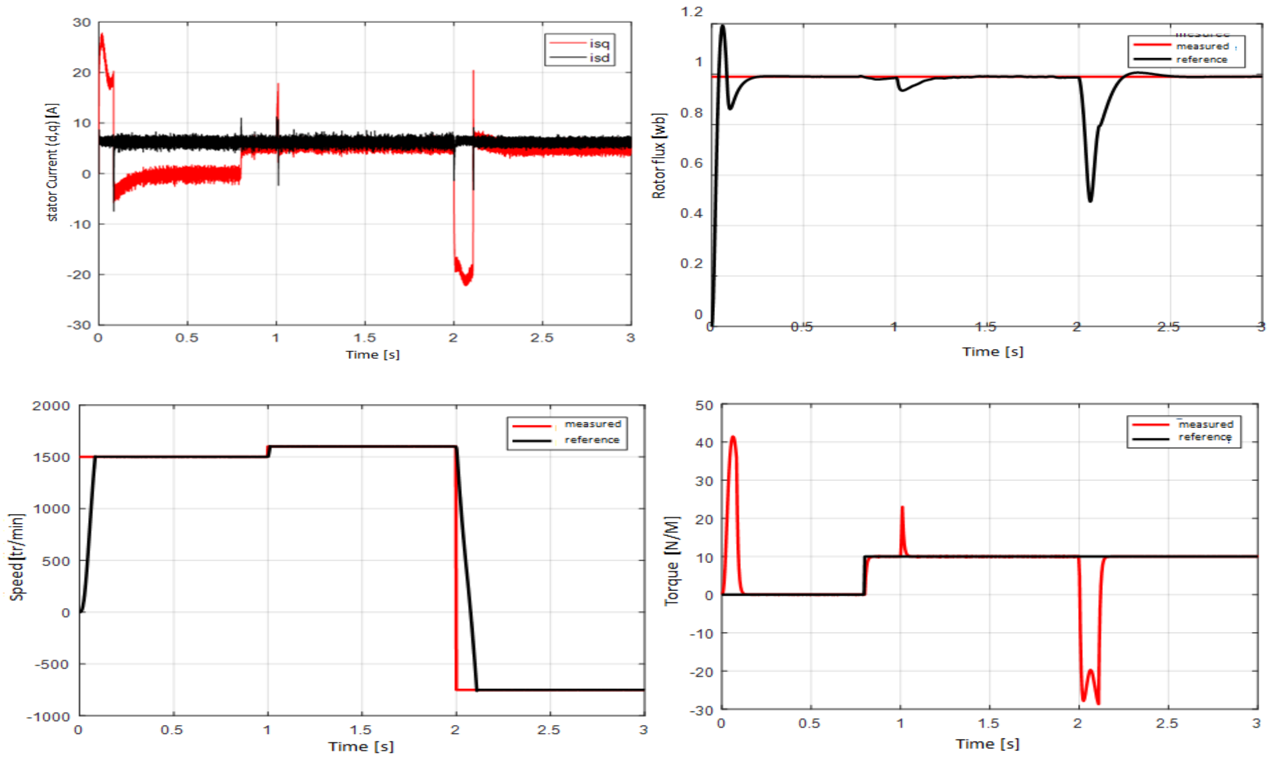

Fig. 2 Simulation results of vector control on a IM by the PI controller.

We note that the speed reached its nominal value with good dynamics and no static error. At the time of application, the load torque (Tr = 10 N.m) with a time (t = 0.8 s), the speed decreased, but it recovers again without static error. The rotor flux components show good flux control with successful decoupling, the torque is quickly controlled in the transient regime.

The emergence of the peaks and are not large in the stator phase currents and in the torque as well as in the rotor fluxes during the speed reversal and especially during the application of the load torque in the time (t = 0.8 s) with a load (Tr = 10 N.m).

4.2 Fuzzy logic speed control of the asynchronous machine

The distribution and especially the number of membership functions over the universe of discourse is very delicate because the computation time of the algorithm must be taken into account during the practical implementation.
For the input fuzzification phase We have selected the same triangular and trapezoidal membership functions for the input and output variables divided into five or seven symmetric and equidistant subsets Fig.3 and Fig.4. This choice allows an easy implementation and fuzzification step because it does not require a large computational time when evaluated in real time.

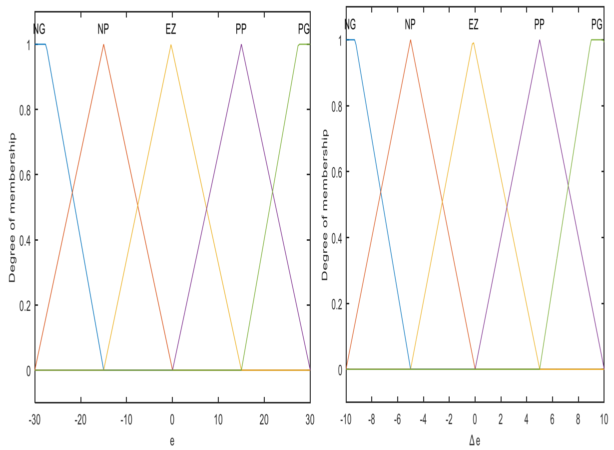

Fig. 3 Membership functions and universe of discourse for the input variables for (5*5) rules.

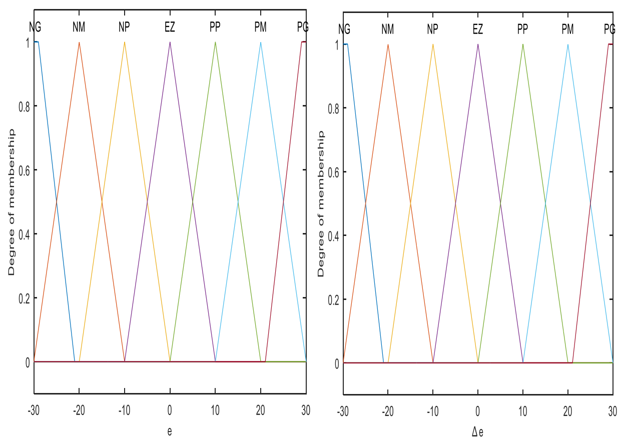

Fig. 4 Membership functions and universe of discourse for the input variables for (7*7) rules.

We have a closed-loop system of FLC regulated speed, we can establish the control rules, which link the output with the inputs, according to our basis on expertise. By offering the inputs of e and Δe which concerns the two cases (5*5) and (7*7) , there are five or seven fuzzy sets in two methods, this implies twenty-five or forty-nine successively possible combinations of these inputs, and thus twenty-five or forty-nine rules.

Table (2): Table of twenty-five rules.

Δe \ e	*NG*	*NP*	*EZ*	*PP*	*PG*
NG	*NG*	*NG*	*NG*	*NP*	*EZ*
NP	*NG*	*NG*	*NP*	*EZ*	*PP*
EZ	*NG*	*NP*	*EZ*	*PP*	*PG*
PP	*NP*	*EZ*	*PP*	*PG*	*PG*
PG	*EZ*	*PP*	*PG*	*PG*	*PG*

Table (2): Table of forty-nine rules.

Δe \ e	*NG*	*NM*	*NP*	*EZ*	*PP*	*PM*	*PG*
NG	*NG*	*NG*	*NG*	*NG*	*NM*	*NP*	*EZ*
NM	*NG*	*NG*	*NG*	*NM*	*NP*	*EZ*	*PP*
NP	*NG*	*NG*	*NM*	*NP*	*EZ*	*PP*	*PM*
EZ	*NG*	*NM*	*NP*	*EZ*	*PP*	*PM*	*PG*
PP	*NM*	*NP*	*EZ*	*PP*	*PM*	*PG*	*PG*
PM	*NP*	*EZ*	*PP*	*PM*	*PG*	*PG*	*PG*
PG	*EZ*	*PP*	*PM*	*PG*	*PG*	*PG*	*PG*

For defuzzification we use The centre of gravity method in order to see the variation of the reference electromagnetic torque. Where the strict value ΔC_e^* is taken from the geometric centre of the output fuzzy variable. Its discretized equation is given by:

$$\Delta C_e^* = \frac{\sum_{i=1}^{n} \Delta C_e(x_i)\mu\Delta C_e(x_i)}{\sum_{i=1}^{n} \mu\Delta C_e(x_i)} \quad (17)$$

For the simulation, we have carried out the results according to the regulation of the parameters of the corrector which are represented in table (3):

Table (3): FLC controller parameters used.

Regulator	*K*
Gain of the error "K_e"	*0.013*
Gain of the error derivative "$K_{\Delta e}$"	*2e-05*
Output gain "K_{Ce-ref}"	*8900*

For the regulation of i_{sd} and i_{sq} currents, it is the same as for the PI regulator.
Here is the block diagram of the simulation of an asynchronous machine controlled by the IFOC technique and with fuzzy logic controller.

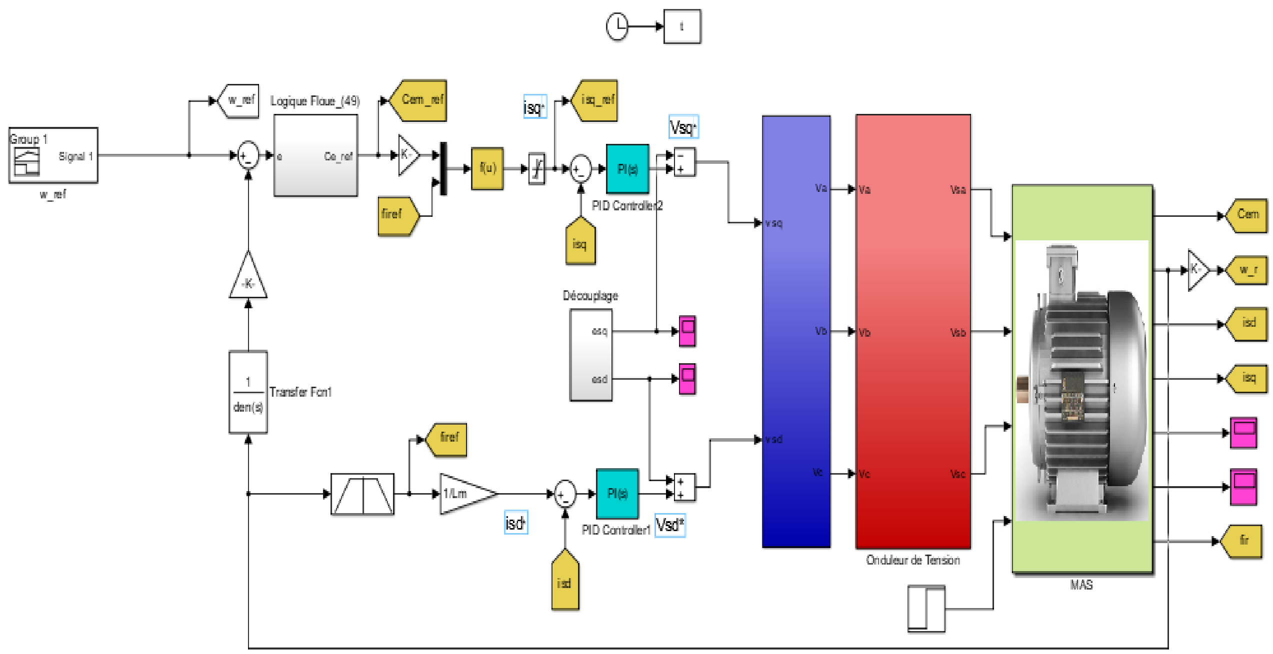

Fig. 5 Block diagram of the simulation of an induction motor controlled by the IFOC technique and with fuzzy logic controller.

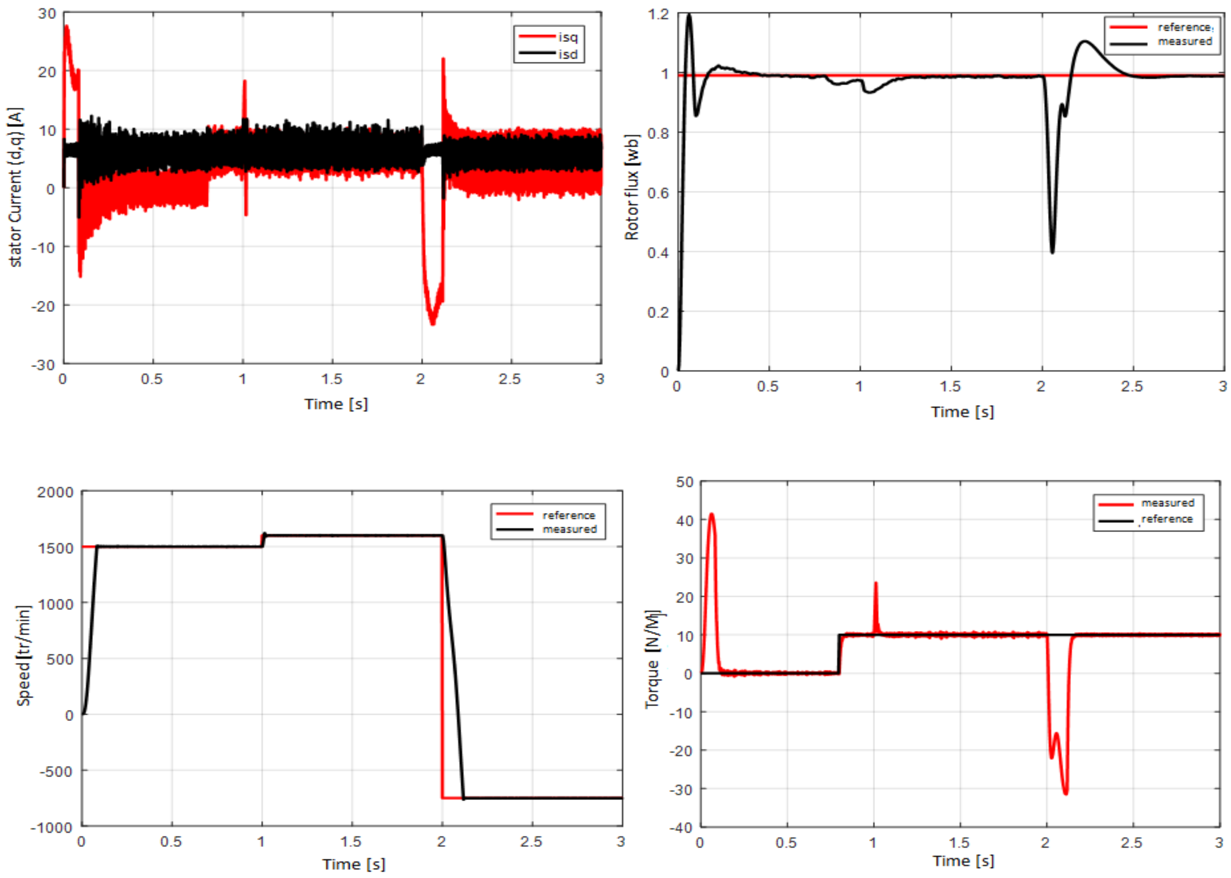

Fig. 6 Simulation results of the IFOC control of a IM by the FLC controller.

The simulation results obtained represent an improved dynamic response at the velocity level. The latter reaches its reference in a response time of 0.09s. On the other hand, the other dynamic responses evolve almost according to the same pattern. The control shows that it is insensitive to the application of the resistive load.

In these results, the decoupling between the electromagnetic torque and the flux during the application of the load (Tr = 10 N.m) over a period of (t = 0.8 s) is quickly rejected by the fuzzy speed controller. On the other hand, the ripples observed during the application of the load torque degraded the stability of the control.

The stator current curve is quasi sinusoidal, because the introduction of a load torque in (Tr = 10) N.m causes an increase in the current.

4.3 Application of neural networks to the induction motor:

4.3.1 Preparation of training data (input-output):

We have chosen the best results obtained when estimating the rotation speed of an IM regulated by fuzzy logic. Thus, 60001 samples per variable are available for the supervisor. After preparing the training base, 70% of the data were retained to be used for the supervised learning of the network, 15% for the validation of the network, and the remaining 15% were retained for the learning test.

4.3.2 Choice of neural network topology:

The choice of the neural network architecture is delicate, as there is no methodology for calculating the number of hidden layers or neurons per layer. We therefore worked by trial and error. Firstly, we opted for structures with a single hidden layer and a reduced number of neurons. Each time, the performance of the network is evaluated, and if the results are not acceptable, the number of neurons is gradually increased until the desired performance is obtained. For the activation functions, we used tangent-sigmoid functions (tansig, in Matlab) for the neurons of the hidden layers, and linear activation functions for the output of the network (purline).

4.3.3 Choice of the learning algorithm:

The last step is the choice of the learning algorithm. We have chosen the back-propagation error learning method. The algorithm chosen is the gradient descent (traingd). As regards the performance indices: the mean square error (mse) to be minimised, and the regression value R which measures the correlation between the outputs and the targets (desired outputs).

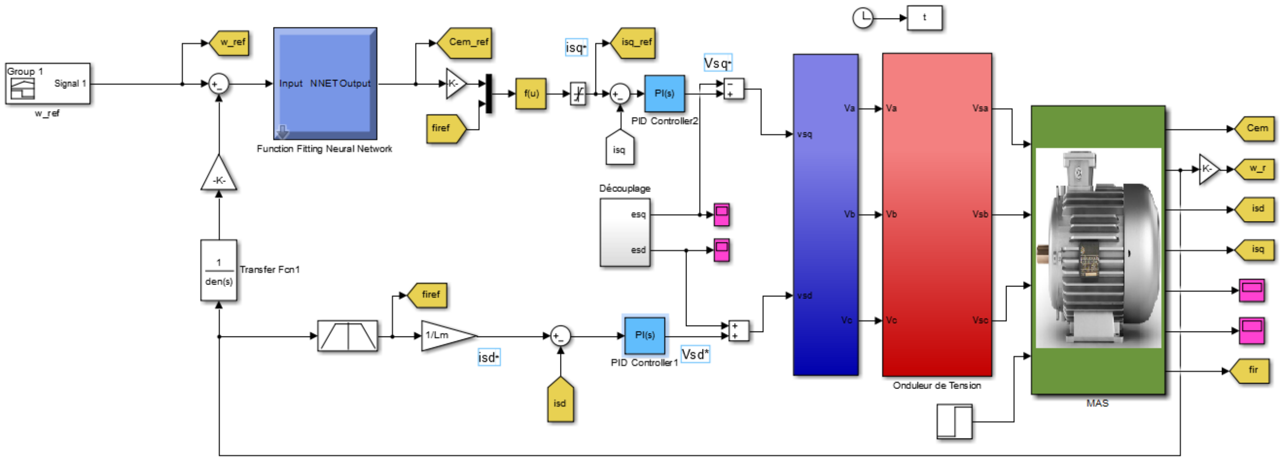

Fig. 7 Block diagram of the simulation of induction motor controlled by the IFOC technique and with neural network controller.

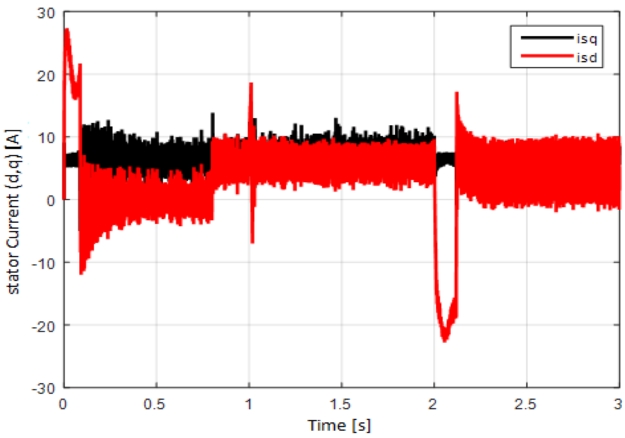

(a)

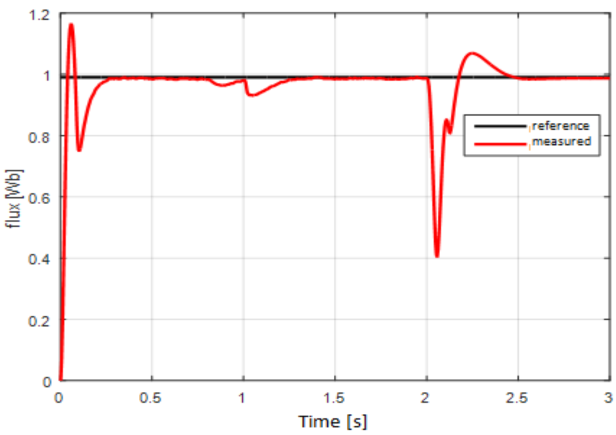

(b)

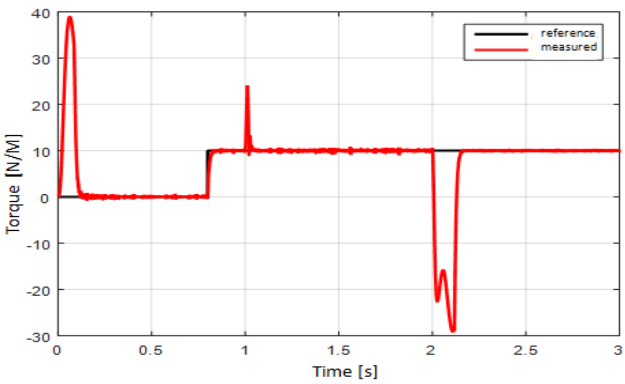

(C)

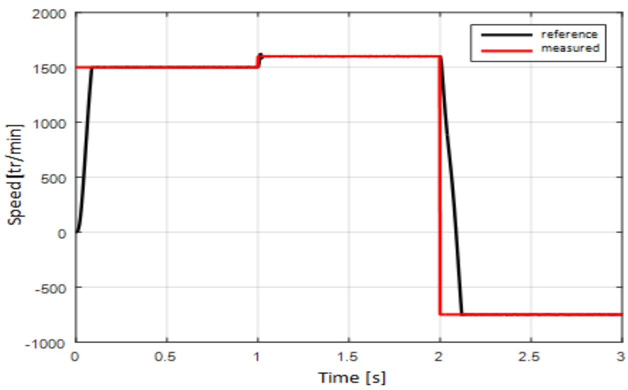

(d)

Fig. 8 (a, b, c and d). The IFOC control of an induction motor by neural network

hey all show the speed, torque, flux and stator current estimated by the ANN at no load or when applying a load. The speed behavior is presented in ***Fig. 8* (d),** when the load is equal to zero at t=0s and when applying a load of 10 N.m at t=0.8s the measured speed gradually reaches the reference speed (faster) and stabilizes at this reference value.

The electromagnetic torque curve illustrated in ***Fig.* 8(c)** shows that a strong current demand between t=0s and t=0.1s (start-up) after which the torque quickly returns to its reference value. It takes the zero value as soon as the speed stabilizes.

In the initial conditions of the load i.e. t=0, the amplitudes of the currents are shown in ***Fig. 8* (a),** when the load is at t=0.8s the stator currents are instantaneously increased.

t can be seen that the flow ***Fig. 8*** *(*b) is slightly disturbed when the torque varies.

The most interesting conclusion of all the tests carried out is that the motor response and that estimated by the network are quite similar and that there is almost no error in the steady state. This shows the ability of the model to generalize and adapt to situations not envisaged in the training phase.

4.3.4 Comparisons between regulators (PI, FLC, RNA)

Report on the results obtained in the previous section, concerning the control of the regulators (PI, FLC, and RNA). The results announced as follows:

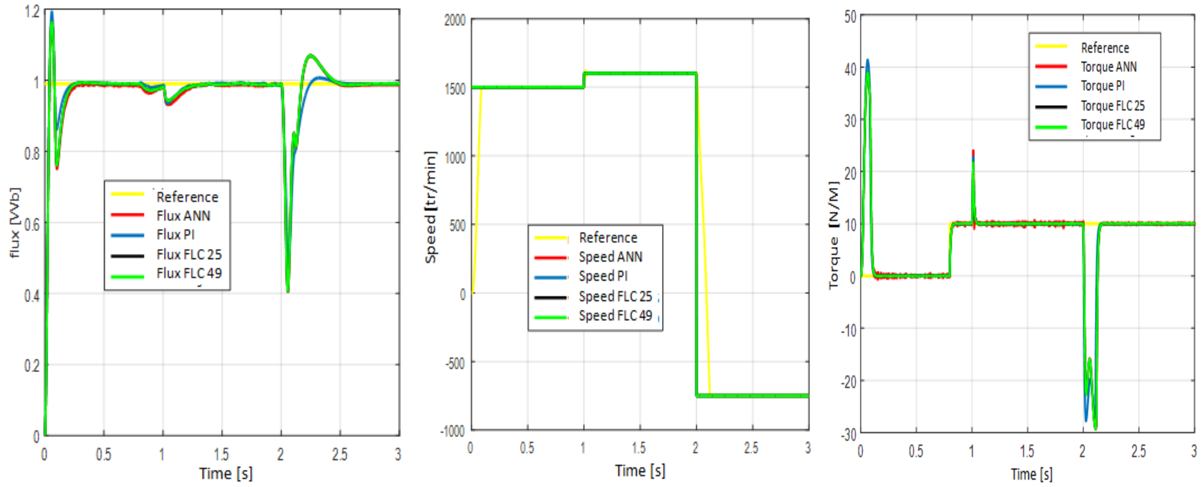

Fig. 9 Vector control results for all PI, FLC, and RNA controllers.

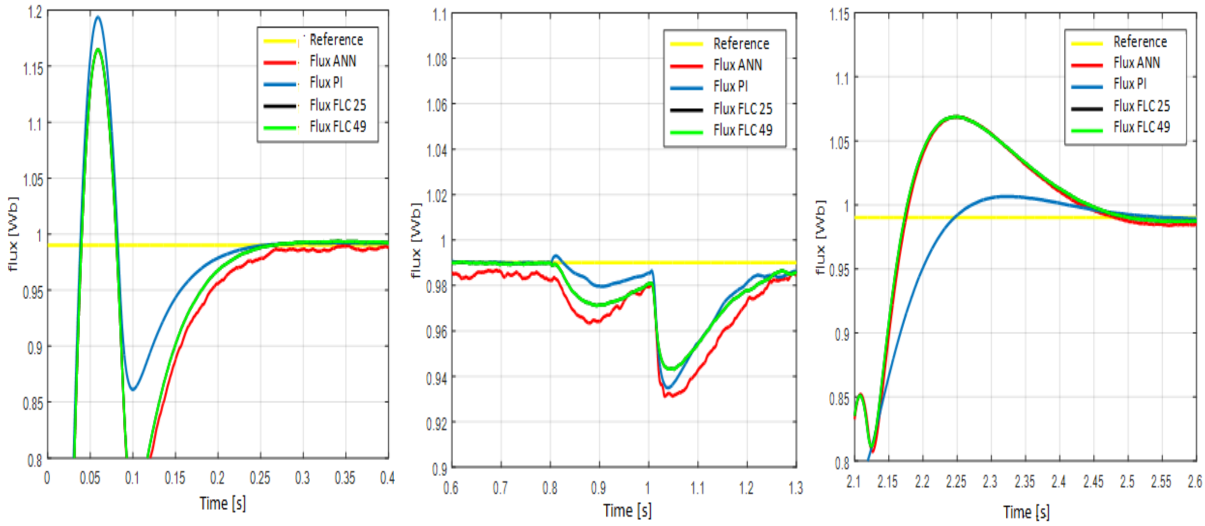

Fig. 10 Zoom of the flux for the different controllers.

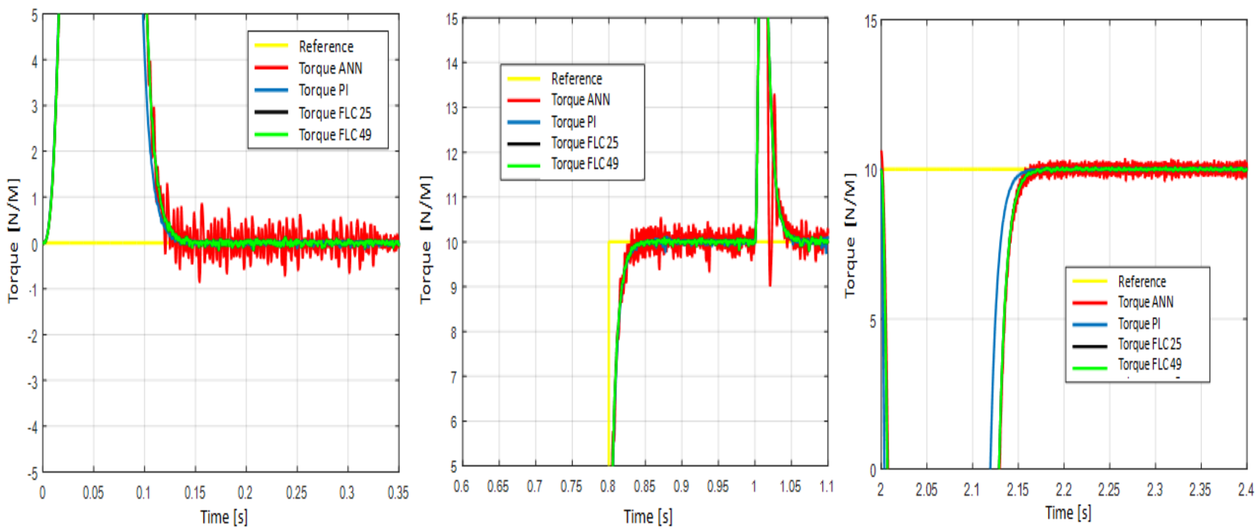

Fig. 11 Torque zoom for the different controllers

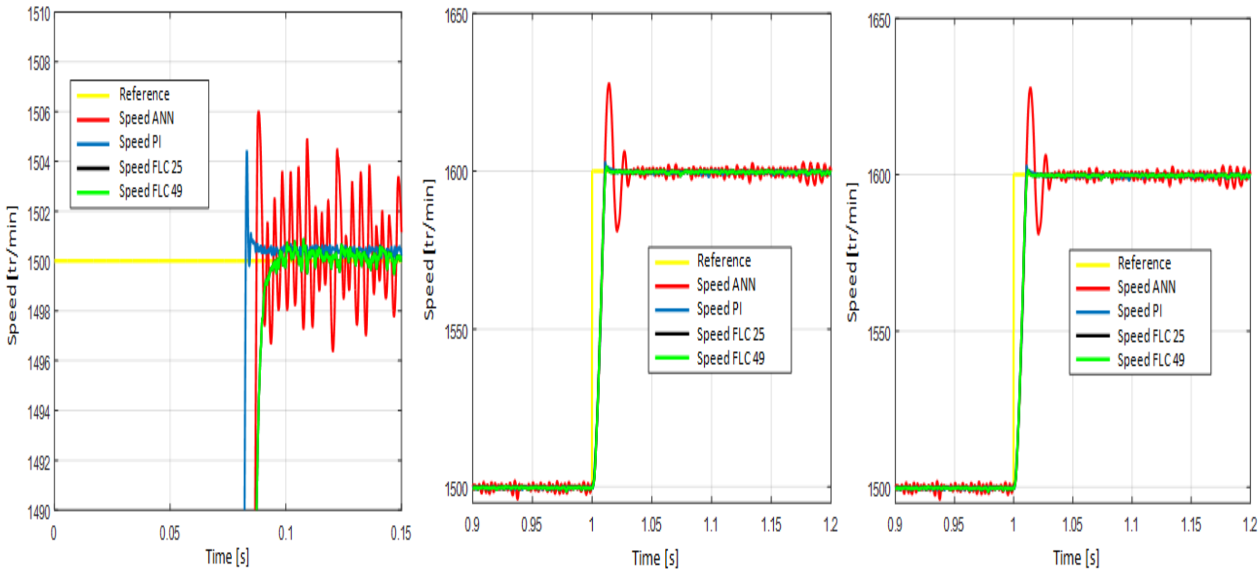

Fig. 12 Speed zoom for the different controllers.

After getting the MATLAB results, we can compare the controllers (classical PI, fuzzy controller, neural network) according to parameters to judge the best one. The comparison is done by the following table:

Table (4): Comparison between the different controllers

regulator	Proportional-Integral	Fuzzy Logic	Neuron Network
Response time	Faster than others (RN and FL)	Fast response and better than others (RN and PI)	Acceptable response compared to FL and better than PI
Performance	Acceptable performance	Acceptable performance	High performance
Robustness	Robust	Very robust	Less robust
Fidelity	Reliable	Very faithful and reliable	Faithful
Stability	Average stability	Very stable	Average stability
Defluxing	Acceptable deflection	Good deflection	Acceptable deflection

5 Conclusion

Despite the positive aspects that characterise the PI controller, it is difficult to master its role at times. The field of fuzzy logic control has become very important, thanks to its ability to process certain information, its importance lies in its high accuracy, fast dynamic response, stability, simplicity of design and implementation, and robustness to the variation of internal or external parameters. Artificial neural networks can be used to design digital controllers that can maintain high dynamic performance of the machine even with the problem of detuning, they are able to mimic the behaviour of any complex non-linear system.

6 References

[1]*SABATE, Victor. "Traction électrique ferroviaire: Convertisseurs et moteurs." Techniques de l'ingénieur. Génie électrique 12. D5502 (1998).*

[2]*Mohamadian M. , Nowicki E. , Ashrafzadeh F. , Chu A. , Sac hdeva R. , Evanik E. Un nouveau contrôleur de réseau neuronal et sa mise en œuvre DSP efficace pour les entraînements de moteurs à induction à commande vectorielle IEEE Trans. Ind. Appl. , 39 (6) (2003) , p. 1622 - 1629*

[3] *Rashid MH Power circuits électroniques, dispositifs et applications. ISBN: 978-81-317-0246-8.*

[4] *Blaschke, Felix. "The principle of field orientation as applied to the new transvector closed-loop control system for rotating-field machines," Siemens review, 1972.*

[5] *L Baghli, « Modélisation et Commande des Machines Asynchrone », Cours de Commande IUFM de Lorrain UHP, 03/04.*

[6] Grellet, Guy, and Guy Clerc. Actionneurs électriques. Éditions Eyrolles, 1997.

[7] Benoit, R. Bruno, F. Philippe, D. Jean paul, H. (2007). «*Commande vectorielle de la machine asynchrone - Désensibilisation et optimisation par la logique floue* », Edition TECHNIP 27 rue Ginoux, 75737 PARIS Cedex 15, FRANCE.